Optimal Bayesian Resampling for OFDM Signaling Over Multi-scale Multi-lag Channels

Sajjad Beygi
University of Southern California
beygihar@usc.edu

Srinivas Yerramalli
University of Southern California
srinivas.yerramalli@usc.edu

Urbashi Mitra
University of Southern California
ubli@usc.edu

ABSTRACT

Underwater acoustic (UWA) communication channels suffer from long delay spreads and significant Doppler effects. Such channels are also ultrawideband in nature. Thus, the typical UWA distortion can be well-described by a multi-scale multi-lag (MSML) channel model. Many UWA communication systems employ resampling by a single-scale at the front-end to compensate for the scale effects of UWA channels. In this paper, the optimal resampling factor for OFDM signaling over MSML channels is investigated from a Bayesian perspective. The resampling factor is selected to minimize the inter-carrier interference resulting from the MSML channel. The exact interference power is computed, but is intractable for optimization, thus an upper bound is employed for optimization. Numerical results verify the tightness of the bound and the Bayesian approach is compared to deterministic methods previously derived for resampling in MSML channels.

Categories and Subject Descriptors

H.4 [**Information Systems Applications**]: Communication Applications; C.3 [**Special-purpose and Application Based Systems**]: Signal Processing Systems

General Terms

Underwater acoustic communications, OFDM, Resampling.

Keywords

Multiscale-Multilag channel, Resampling, Intercarrier Interference (ICI).

This research has been funded in part by ONR N00014-09-1-0700, NSF CNS-0832186 and NSF CCF-1117896.

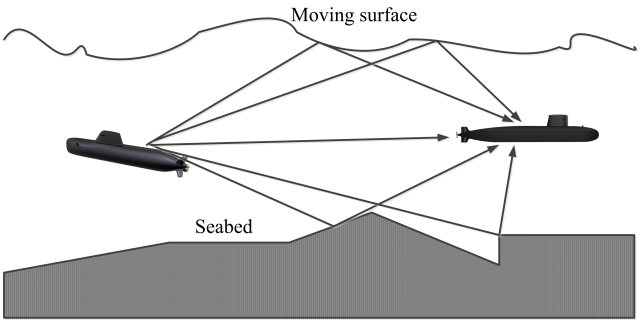

Figure 1: Mobile underwater acoustic communication channel.

1. INTRODUCTION

Environmental, surveillance and military applications drive the need for high speed underwater acoustic communications. Achieving this goal is challenged by the low speed of propagation of sound in water, as well as the relatively high Doppler induced by mobility. Despite these challenges, there is strong interest in Orthogonal Frequency Division Multiplexing (OFDM) as a signalling scheme for underwater acoustic communications [1, 2, 3]. The subcarrier orthogonality of OFDM that is retained in linear-time-invariant channels is typically lost in the presence of time-variation [2, 3, 4, 5, 6]. In a narrowband wireless communications, the effect of Doppler distortion can be modeled as a frequency offset or via time-varying multipath coefficients [7, 8]. However, in wideband signalling environments such as UWA communications, the Doppler distortion on each path results in time scaling (compression or dilation) of the signal [4, 9, 11]. Thus the received signal can be well-modeled by a multi-scale multi-lag (MSML) channel [4].

Common front-end processing used to mitigate the effects of Doppler scaling includes resampling to eliminate the dominant time scale component [3, 4, 14]. For single-scale channels, resampling is optimal [4], eliminating the inter-carrier interference (ICI) induced by mobility. While, resampling alone is suboptimal for MSML channels [4], it remains an effective technique for mitigating the effects of multiple scales. Thus we presume such a two-stage approach (resampling followed by further compensation for residual ICI) and investigate optimal resampling from a Bayesian perspective.

Prior work on resampling factor estimation focused on deterministic models. In [13, 14], the time scale factor is estimated by measuring the differences between transmitted and received packet durations. Our prior work [4], first determined the optimal resampling parameter under perfect channel state information at the receiver and then presented blind and pilot aided estimation algorithms for the optimal resampling parameter. A scenario with very small time scales is considered in [2] and its effect modeled as a carrier frequency offset. A joint frequency offset and channel estimation algorithm is then proposed to estimate the desired parameters.

In this paper, we investigate optimal resampling for an MSML UWA channel under a probabilistic model for the channel gain, delay and time scale on each path. We assume only knowledge of the second order statistics of the channel parameters. We first accurately compute the ICI caused by a given resampling factor as a function of the statistics of the channel. The optimal resampling parameter is the one which minimizes the total ICI for the OFDM signaling. Minimizing the exact ICI power has proven to be analytically intractable. To overcome this difficulty, we first compute a tight upper bound on the ICI and the optimal resampling parameter is estimated by minimizing the upper bound. Under the assumption of independent channel gains on each path and assuming the same probability distribution for the time scale on each path, we show that the optimal resampling parameter is only a function of the first and second order statistics of the time scale parameter and is entirely determined by the distribution of the time scale. Numerical simulations are then presented to verify the tightness of the ICI upper bound and demonstrate the gains that can be obtained by using statistical information about the channel.

The rest of this paper is organized as follows. The signal model for OFDM based UWA transmission is presented in Section 2. Section 3 presents the resampling operation and the evaluates the exact ICI. An upper bound for the ICI is presented in Section 4 and Section 5 evaluates the upper bound for the channel model previously described. Section 6 presents numerical simulations to verify the tightness of the upper bound and provides a comparison with other resampling techniques and Section 7 concludes this paper.

Notations: Expectation is denoted by $E\{.\}$, $|.|$ and $(.)^*$ denotes the absolute value and conjugation operator respectively. The Fourier transform operator is given by $\mathcal{F}\{.\}$ and differentiation with respect to x operator with $\frac{\partial}{\partial x}$.

2. SYSTEM MODEL

2.1 Transmitted Signal

The transmitted passband OFDM signal is given by

$$x(t) = \sum_{k=0}^{N-1} x_k e^{j2\pi f_k t}, \qquad (0 \le t \le T), \tag{1}$$

where T is the OFDM symbol duration, N is the number of sub-carriers, x_k is the data modulated onto the k^{th} subcarrier; f_k is the k^{th} subcarrier frequency, where $f_k = f_{min} + k\Delta f$; $\Delta f = \frac{1}{T}$ is the sub-carrier spacing; f_{min} is minimum carrier frequency; and $B = N\Delta f$ is the bandwidth of the system. A rectangular pulse shape over the interval $t \in [0, T]$ is employed.

2.2 Underwater Channel Model

The linear time-varying (LTV) channel is characterized by the impulse response, $h(t, \tau)$, which denotes the response of the channel at time t to an impulse at time $t - \tau$. The received signal after passing through a LTV channel can be written as,

$$y(t) = \int_{-\infty}^{+\infty} h(t, \tau) x(t - \tau) d\tau + \nu(t), \tag{2}$$

where $\nu(t)$ is assumed to be additive, white Gaussian noise. The ratio v/c, where v is the relative velocity between the transmitter and the receiver and c is the speed of propagation of sound in water, is very large compared to that of terrestrial radio communications. As a result, the typical narrowband assumptions invoked for terrestrial radio cannot be employed in the UWA scenario. In particular, mobility induces time scaling and not Doppler shifts [6]. The time scale is given by $a = \frac{v}{c} cos\theta$ where θ is the angle-of-arrival relative to the direction of travel [7]. Thus, the scale parameter on a path can take any value from $[-\frac{v}{c}, \frac{v}{c}]$.

The received signal is an aggregation of several scaled copies of the delayed and attenuated transmitted signal aggregately represented by the MSML channel model:

$$h(t, \tau) = \sum_{n=1}^{M} h_n \delta\left(\tau - \tau_n(t)\right), \quad \tau_n(t) = \tau_n - a_n t, \tag{3}$$

where h_n, τ_n, and a_n are the channel path gain, path delay, and time scaling on the n^{th} path, respectively (see [6], [5] and [12] for a more detailed development and analysis of such channel models). We shall model the channel parameters as random variables. We assume that the parameters a_n, τ_n, and h_n are mutually independent, the path gains are zero mean, i.e. $E\{h_n\} = 0$ with known second moment. Note that this model encompasses the Rayleigh fading model of channel taps [15]. The case of channels with non-zero means (Ex: Rician fading) is not in the scope of this paper. We also note that for the purposes of computing ICI power, the knowledge of second moment of the channel gains is sufficient and is independent of the distribution. Next, we assume the τ_n is distributed uniformly over $[0, T_d]$, where, T_d is the multipath delay spread [16]. The distribution of the time scales on each tap will be discussed later in the paper. From (1), (2) and (3), the received signal can be expressed as

$$y(t) = \sum_{n=1}^{M} \sum_{k=0}^{N-1} h_n x_k e^{j2\pi f_k (t - (\tau_n - a_n t))} + \nu(t), \tag{4}$$

which can be factored as

$$y(t) = \sum_{k=0}^{N-1} \underbrace{\left(\sum_{n=1}^{M} h_n e^{-j2\pi f_k(\tau_n - a_n t)} \right)}_{h_k(t)} x_k e^{j2\pi f_k t} + \nu(t)$$

$$= \sum_{k=0}^{N-1} h_k(t) x_k e^{j2\pi f_k t} + \nu(t). \quad (5)$$

In (5), $h_k(t)$ is the time-varying channel frequency response as experienced by the k^{th} sub-carrier. The k^{th} subcarrier experiences a frequency offset of $f_k a_m$ on the m^{th} path and this frequency shift changes linearly with the sub-carrier index.

3. RESAMPLING

As previously noted, mobility induces a scaling (dilation/ compression) of the transmitted waveform in these wideband channels. For single-scale channels, resampling (or rescaling of the waveform with respect to time) is an effective compensation for Doppler scaling.

In this section, we characterize the effect of resampling on MSML signals. To provide some intuition to this effect, we first consider the scenario with single scale channels and then we discuss multi-scale channels.

3.1 Single Scale, Multi-Lag Channels

For this scenario we have

$$\tau_n(t) = \tau_n - at,$$

thus, the time domain single-scale received signal $y(t)$, when source signal $x(t)$ is transmitted, is

$$y(t) = \sum_n h_n x\left((1+a)\,t - \tau_n\right) + \nu(t).$$

If the scaling parameter, a, is known, then the received signal can be dilated/compressed by the inverse scaling factor. Proper resampling completely eliminates ICI in this scenario [11] and symbol-by-symbol processing is optimal.

3.2 MSML Channels

When the channel paths have different time scales, a_n, the time domain multi-scale received signal $y(t)$ is given by

$$y(t) = \sum_n h_n x\left((1+a_n)\,t - \tau_n\right) + \nu(t).$$

As we can see in the case of multiple, distinct, scales, symbol-by-symbol processing is not optimal [4], and the frequency-dependent Doppler scales introduce strong ICI if effective Doppler compensation is not performed. For this channel, resampling with the factor b, results in the received signal

$$y_b(t) = y\left(\frac{t}{1+b}\right)$$

$$= \sum_{k=0}^{N-1} h_k\left(\frac{t}{1+b}\right) x_k e^{j2\pi f_k\left(\frac{t}{1+b}\right)} + \nu\left(\frac{t}{1+b}\right) \quad (6)$$

Our goal herein is to determine the optimal single-scale resampling factor for MSML channels that will be yield the smallest ICI.

3.3 ICI Power After Resampling

We now compute an exact expression for the ICI power in OFDM-based UWA systems given that a single resampling operation is performed at the receiver. Assuming perfect time synchronization, the received signal after resampling with the factor b and projection onto the m^{th} subcarrier can be expressed as

$$y_m = \frac{1}{T}\int_0^T y_b(t) e^{-j2\pi f_m t} dt. \quad (7)$$

After substituting $y_r(t)$ form (6) in (7), we have

$$y_m = \left(\frac{1}{T}\int_0^T h_m\left(\frac{t}{1+b}\right) e^{\frac{-j2\pi f_m bt}{1+b}} dt \right) x_m +$$

$$\underbrace{\sum_{k\neq m} \left(\frac{1}{T}\int_0^T h_k\left(\frac{t}{1+b}\right) e^{\frac{-j2\pi f_k bt}{1+b}} e^{-j2\pi(f_m - f_k)t} dt \right) x_k}_{\text{ICI term induced by the MSML channel}} + \nu_m, \quad (8)$$

where ν_m is additive white Gaussian noise. Eqn. (8) can be rewritten as $y_m = c_m x_m + \sum_{k\neq m} c_{km} x_k + \nu_m$ where

$$c_{km} \triangleq \frac{1}{T}\int_0^T \mu_k(t) e^{-j2\pi(f_m - f_k)t} dt,$$

and $\mu_k(t) = h_k(\frac{t}{1+b}) e^{-j2\pi f_k(\frac{bt}{1+b})}$.

With (8), we can now obtain an expression for the ICI power. Since the transmitted symbols have unit power and are independent and zero-mean, it is easy to show that the ICI power on the m^{th} subcarrier is given as

$$P_{ICI}^{(m)} = E\left\{ \left| \sum_{k\neq m} c_{km} x_k \right|^2 \right\} = \sum_{k\neq m} E\left\{ |c_{km}|^2 \right\}. \quad (9)$$

From [17] (Chapter 10, 10-28), it can be further shown that

$$E\left\{ |c_{km}|^2 \right\} = \int_{-1}^{1} C_k(T\lambda)\left(1 - |\lambda|\right) e^{j2\pi(k-m)\lambda} d\lambda, \quad (10)$$

where $C_k(\tau)$ is the autocorrelation of $\mu_k(t)$, namely

$$C_k(\tau) = \frac{1}{2} E\{\mu_k(t+\tau)\mu_k^*(t)\}. \quad (11)$$

Substituting the expression for $h_k(t)$ from (5), we have

$$\mu_k(t) = \sum_{n=1}^{M} h_n e^{-j2\pi f_k \tau_n} e^{j2\pi f_k \frac{a_n - b}{1+b} t}. \quad (12)$$

Using (12), we obtain the following expression for the autocorrelation function (11):

$$C_k(\tau) = \frac{1}{2} E\left\{ \sum_{n=1}^{M}\sum_{m=1}^{M} h_n h_m^* e^{-j2\pi f_k(\tau_n - \tau_m)} \times e^{j2\pi f_k(\varphi_n - \varphi_m)t} e^{j2\pi f_k \varphi_n \tau} \right\}, \quad (13)$$

where $\varphi_n = \frac{a_n - b}{1+b}$. Due to statistical independence between the channel parameters, we can rewrite (13) as,

$$C_k(\tau) = \frac{1}{2}\sum_{n=1}^{M} E\{|h_n|^2\} E_a\{e^{j2\pi f_k \frac{a-b}{1+b}\tau}\}. \quad (14)$$

As mentioned before $a = \frac{v}{c}cos\theta$, thus we can rewrite (14) as

$$C_k(\tau) = \Upsilon_h e^{-j2\pi f_k \frac{b}{1+b}\tau} E_\theta\{e^{j2\pi \frac{\bar{f}_k \tau}{1+b}\cos\theta}\}, \quad (15)$$

where

$$\Upsilon_h = \frac{1}{2}\sum_{n=1}^{M} E\left\{|h_n|^2\right\}, \quad (16)$$

and $\bar{f}_k = \frac{v}{c} f_k = \beta f_k$. For the sake of simplicity, we define the normalized correlation function as

$$g(x) = \Upsilon_h e^{\frac{-j2\pi b}{(1+b)\beta}x} E_\theta\{e^{\frac{j2\pi x}{1+b}\cos\theta}\}, \quad (17)$$

which is related to the autocorrelation function $C_k(\tau)$ as

$$C_k(\tau) = g(\bar{f}_k \tau). \quad (18)$$

From (18), we can rewrite $C_k(T\lambda)$ as

$$C_k(T\lambda) = g(\bar{f}_k T\lambda) = \int_{-\infty}^{+\infty} G(f) e^{j2\pi f(\bar{f}_k T\lambda)} df, \quad (19)$$

where $G(f)$, the normalized Doppler spectrum, is the Fourier transform of $g(x)$:

$$\begin{aligned} G(f) &= \int_{-\infty}^{+\infty} g(x).e^{-j2\pi fx} dx \\ &= \int_{-\infty}^{+\infty} \Upsilon_h e^{\frac{-j2\pi b}{(1+b)\beta}x} E_\theta\left\{e^{\frac{j2\pi x}{1+b}\cos\theta}\right\}.e^{-j2\pi fx} dx \\ &= E_\theta\left\{\int_{-\infty}^{+\infty} \Upsilon_h e^{\frac{-j2\pi b}{(1+b)\beta}x} e^{\frac{j2\pi x}{1+b}\cos\theta} e^{-j2\pi fx} dx\right\}. \end{aligned} \quad (20)$$

Using $\mathcal{F}\{e^{j2\pi\varepsilon x}\} = \delta(f-\varepsilon)$, where $\delta(.)$ is the Dirac delta function, in (20) we have,

$$G(f) = \Upsilon_h E_\theta\left\{\delta\left(f + \frac{b}{(1+b)\beta} - \frac{\cos\theta}{1+b}\right)\right\}. \quad (21)$$

Based on the scaling property of the Dirac delta function, we have

$$\begin{aligned} G(f) &= \Upsilon_h(1+b) E_\theta\left\{\delta\left(\cos\theta - (1+b)f - \tfrac{b}{\beta}\right)\right\} \\ &= \begin{cases} \Upsilon_h(1+b)\left\{\frac{p_\theta(\Psi(f)) + p_\theta(-\Psi(f))}{\sqrt{1-\left((1+b)f+\frac{b}{\beta}\right)^2}}\right\} & f_l \le f \le f_u \\ 0 & else \end{cases} \end{aligned} \quad (22)$$

where $\Psi(f) = \cos^{-1}\left((1+b)f + \frac{b}{\beta}\right)$, $f_u = \frac{\beta - b}{\beta(1+b)}$, and $f_l = \frac{-(\beta+b)}{\beta(1+b)}$. The Doppler spectrum only depends on the distribution of the scattering angle θ, i.e., $p_\theta(.)$. Furthermore, the shape of the normalized Doppler spectrum does not depend on $\bar{f}_k$.

Considering (9), (10), (19), and (22), $P_{ICI}^{(m)}$ becomes

$$\begin{aligned} P_{ICI}^{(m)} &= \sum_{k\neq m} \int_{-\infty}^{+\infty} G(f) \\ &\quad \times \left\{\int_{-1}^{+1} e^{j2\pi f(\bar{f}_k T\lambda)}(1-|\lambda|) e^{j2\pi(k-m)\lambda} d\lambda\right\} df. \end{aligned} \quad (23)$$

The integrand with bounds -1 to +1 can further be simplified by exploiting symmetry in the odd and even parts. The odd part equals zero, and the even part can be written as

$$\begin{aligned} P_{ICI}^{(m)} &= \sum_{k\neq m} \int_{-\infty}^{+\infty} G(f) \\ &\quad \times \left\{2\int_{0}^{+1} (1-\lambda)\cos\left(2\pi\left[f(\bar{f}_k T) + (k-m)\right]\lambda\right) d\lambda\right\} df \\ &= \sum_{k\neq m} \int_{-\infty}^{+\infty} G(f)\mathrm{sinc}^2(k-m+f(\bar{f}_k T)) df \\ &= \int_{-\infty}^{+\infty} G(f) S_m(f) df, \end{aligned} \quad (24)$$

where

$$S_m(f) = \sum_{k\neq m} \mathrm{sinc}^2(k-m+f(\bar{f}_k T)). \quad (25)$$

Substituting $\bar{f}_k = \beta(f_c + k\Delta f)$ and $T = \frac{1}{\Delta f}$ in (25), and defining $\alpha \triangleq \frac{f_c}{\Delta f}$ then we can rewrite (25) as

$$S_m(f) = \sum_{k\neq m} \mathrm{sinc}^2\left\{(\beta f + 1)k + (\alpha\beta f - m)\right\}. \quad (26)$$

Thus the exact expression for the ICI power in the m^{th} sub-carrier becomes

$$P_{ICI}^{(m)} = \int_{-\infty}^{+\infty} G(f) S_m(f) df. \quad (27)$$

The total power for the ICI at receiver for all sub-carriers will thus be

$$P_{ICI} = \sum_{m=0}^{N-1} P_{ICI}^{(m)}. \quad (28)$$

The integral in (27) cannot be calculated directly. Therefore, we will calculate an upper-bound for the ICI power. We will then seek to optimize the upper bound via our choice of b.

4. ICI POWER APPROXIMATION

In the following theorem we evaluate an upper bound for $S_m(f)$.

THEOREM 1. *Assume* $f_l = \frac{-(b+\beta)}{\beta(1+b)}$ *and* $f_u = \frac{(\beta-b)}{\beta(1+b)}$, *(i) For* $f_l \le f < 0$

$$S_m(f) \le \frac{1}{1+\beta f} - \mathrm{sinc}^2\left(\beta(\alpha+m)f\right). \quad (29)$$

(ii)For $0 \leq f < f_u$

$$S_m(f) \leq \frac{\left(2\cos\left(\frac{2\pi(\beta\alpha f - m)}{1+\beta f}\right)+1\right)\beta f + 1}{(1+\beta f)^2} - \operatorname{sinc}^2\left(\beta(\alpha+m)f\right). \quad (30)$$

PROOF. The proof is given in Appendix A. □

Since β is much smaller than one ($\approx 10^{-3}$) and b is upper-bounded by β and f is limited to the interval $[f_l, f_u]$, and $-2 \leq f_l \leq -1$ and $0 \leq f_u \leq 1$, thus we can conclude that $\beta f + 1 \approx 1$ and $\cos(\frac{2\pi(\alpha\beta f - m)}{1+\beta f}) \approx \cos(2\pi\alpha\beta f)$, which means that the cosine has nearly $\alpha\beta$ ripples between the 0 and 1 frequencies. Furthermore, $\alpha\beta = \beta f_c T$ is the maximum Doppler shift for the zeroth sub-carrier and this value is usually less than $\frac{1}{2}$. Thus, we anticipate that the upper bounds provided in Theorem 1 will be tight. This will be verified in Section 7.

The second order Taylor series of bounds in the *Theorem 1* are

$$S_m(f) \leq \begin{cases} -\beta f + (\beta f)^2\left[1 + \frac{\pi^2}{3}(\alpha+m)^2\right] & f_l \leq f < 0 \\ \beta f + (\beta f)^2\left[-3 + \frac{\pi^2}{3}(\alpha+m)^2\right] & 0 \leq f \leq f_u \end{cases} \quad (31)$$

Thus, using (31) and (27) we can compute a tight upper-bound for ICI as,

$$P_{ICI}^{(m)} \leq m_1\beta + (m_3 + \frac{\pi^2}{3}m_2(\alpha+m)^2)\beta^2, \quad (32)$$

where parameters the $m_1 = \int_{f_l}^{f_u} |f| G(f) df$, $m_2 = \int_{f_l}^{f_u} f^2 G(f) df$, and $m_3 = \int_{f_l}^{0} f^2 G(f) df - 3\int_{0}^{f_u} f^2 G(f) df$.

5. RESAMPLING ESTIMATION

In this section, first we introduce the K-state modelling of time-scale profile which can be considered as a generalization of two-path modelling [7]. Then the resampling factor b for K-state modelling of time-scale profile is calculated.

K-state model: The scale parameter in an MSML UWA channel on each path can take any value from $-\frac{v}{c}$ to $\frac{v}{c}$. Since the probability of receiving in some direction say θ_i can be larger than others (let p_i be the probability associated with the value θ_i, i^{th} direction of arrival), we can model general distribution $p_a(a)$ as a collection of probable angle-of-arrivals in the discrete points $a_i = \beta cos(\theta_i)$ with probability p_i

$$p_a(a) = \sum_{i=1}^{K} p_i \delta(a - a_i), \quad (33)$$

where p_i is the occurrence probability of time scale a_i . For convenience in computation, we assume $a_1 \leq a_2 \leq ... \leq a_K$. From $p_a(a)$, we can compute $p_\theta(\theta)$ and then $G(f)$ using (21). Considering the K-state model leads to

$$G(f) = \Upsilon_h \sum_{i=1}^{K} p_i \delta(f - f_i), \quad (34)$$

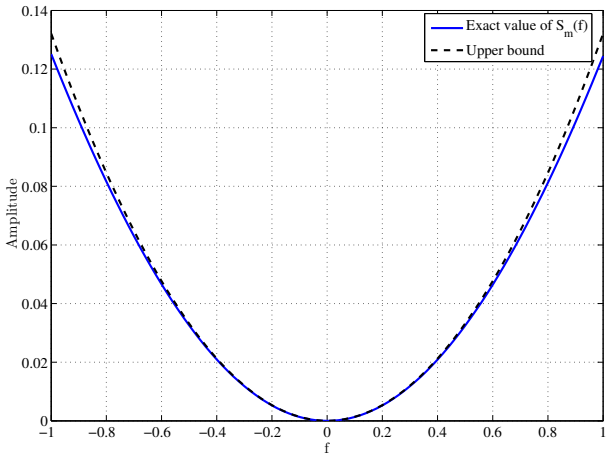

Figure 2: Exact $S_m(f)$ and the proposed upper bound for $\alpha\beta < 0.5$.

where $f_i = \frac{a_i - b}{\beta(b+1)}$. Having $G(f)$ from (34), parameters m_1, m_2, and m_3 in (32) result as following,

$$m_1 = \Upsilon_h \sum_{i=1}^{K} p_i \frac{|a_i - b|}{\beta(1+b)} \quad (35)$$

$$m_2 = \Upsilon_h \sum_{i=1}^{K} p_i \frac{(a_i - b)^2}{\beta^2(1+b)^2} \quad (36)$$

$$m_3 = \Upsilon_h \left\{ \sum_{i_1=1}^{j} p_{i_1} \frac{(a_i - b)^2}{\beta^2(1+b)^2} - 3 \sum_{i_2=j+1}^{K} p_{i_2} \frac{(a_i - b)^2}{\beta^2(1+b)^2} \right\} \quad (37)$$

where $j = \{i | a_i \leq b < a_{i+1}\}$ in (37). A special case of the K-state model is the *uniform K-state model* which occurs when $p_i = \frac{1}{K}$.
In the following we state the optimal b for K-state modelling.

PROPOSITION 1. *If we substitute the values of m_1, m_2, and m_3 from Eq. (35) to (37) in (32) then the optimal value of b which minimizes the upper-bound for K-state modelling is given by*

$$b = \frac{\varsigma\mu_{a^2} + (\varsigma+1)\mu_a + 1 - \Omega_2}{(\varsigma+19)(\mu_a+1) + \Omega_1} \quad (38)$$

where $\mu_a = E\{a\}$, $\mu_{a^2} = E\{a^2\}$, $\Omega_1 = 10\sum_{i=1}^{j}(1+a_i)p_i$, $\Omega_2 = 2\sum_{i=1}^{j}(4a_i^2 + 3a_i - 1)p_i$; $j = \{i | a_i \leq b < a_{i+1}\}$ *and* $\varsigma = \frac{2T_\alpha}{N} - 6$; *and* $T_\alpha = \frac{1}{N}\sum_{m=0}^{N-1}(\alpha+m)^2$.

6. SIMULATION AND DISCUSSION

In this section, we validate our mathematical analysis. We first confirm the approximation of theorem 1. In Figures 2 and 3 we compare the exact value of $S_m(f)$ to the upper bound approximation of $S_m(f)$. These figures confirm that for $\alpha\beta \leq 1/2$ the bound is tight.

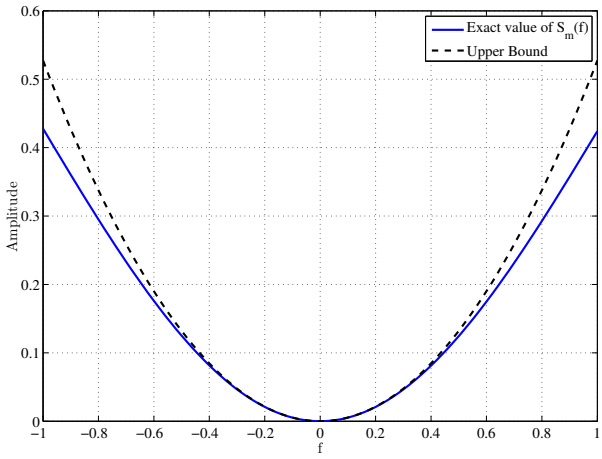

Figure 3: Exact $S_m(f)$ and the proposed upper bound for $\alpha\beta > 0.5$.

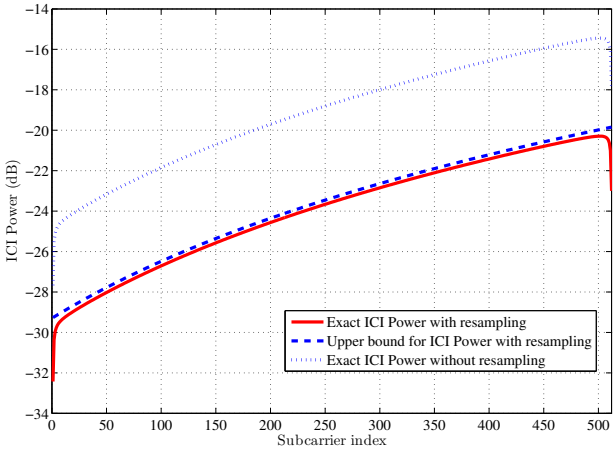

Figure 4: Exact and upper bound for ICI resampling for proposed b in Eq. (38).

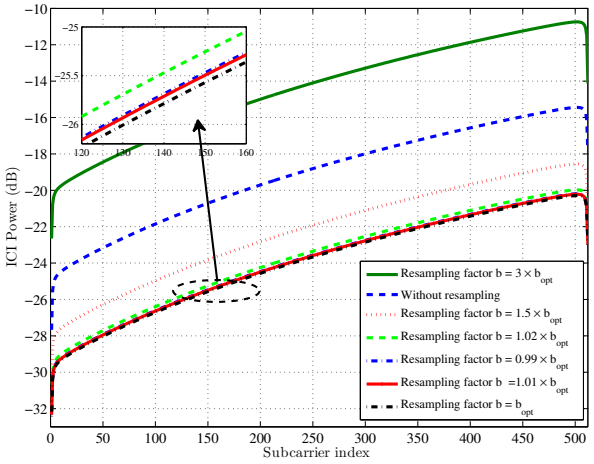

Figure 5: Optimality of computed resampling factor b in Eq. (38).

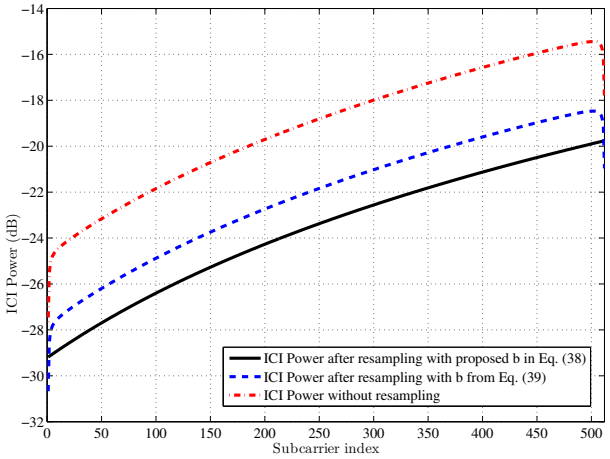

Figure 6: Performance comparison of proposed resampling factor Eq.(38) and resampling factor Eq.(39).

In Fig. 2, we consider $\beta = 5\times10^{-4}$, and $\alpha = \frac{f_c}{\Delta f} \approx 350$. In Fig. 3, $\alpha\beta > 1/2$ for $\beta = 1 \times 10^{-3}$ and we see the expected looseness of the bound. Observe that we can reduce this effect by choosing the symbol duration to be smaller.

We next illustrate the difference between approximated (32) and exact (28) ICI power via simulation. For this experiment, we consider an OFDM transmission system with $N = 512$ subcarriers, $\Delta f = 50Hz$ subcarrier spacing, $f_{min} = 4kHz$, and $\beta = 5 \times 10^{-3}$.

In Fig. 4 the exact ICI power with and without resampling and its bound from (32) are compared. We use the K-state model where $K = 5$, $p_a(a) = \sum_{i=1}^{5} p_i \delta(a - a_i)$ and the a_i are drawn from $\{\beta, 0.1\beta, 0.4\beta, 0.6\beta, 0.2\beta\}$, with $p_i = 0.2$ for all i. In the next experiment, we check the optimality of the computed resampling factor in Proposition 1, Eq. (38). To perform this test, we consider four different values for the resampling factor. One is the optimal value, b_{opt}, computed from (38), as well as $b = 0.99b_{opt}$, $b = 1.01b_{opt}$, $b = 1.02b_{opt}$, $b = 1.5b_{opt}$, and $b = 3b_{opt}$. To compare the values for $b = 0.99b_{opt}$, $b = 1.01b_{opt}$, $b = 1.02b_{opt}$, and $b = b_{opt}$, we also add the magnified part of the plots to the top-left side of figure. As is clear from Fig. 5, b_{opt} gives the best performance, namely the ICI power after resampling with b_{opt} is the smallest in comparison with the other resampling factors. Note, from Fig. 5, it is clear that if the value of resampling factor was chosen wrong (e.g. $b = 3b_{opt}$) then the ICI power value may be more than the case without resampling.

A common way to compute the resampling factor (see e.g. [11], [14], [3], [10] and their references) is to assume a single scale and to estimate the resampling factor as

$$\hat{b} = \frac{T_{pTx}}{T_{pRx}} - 1, \tag{39}$$

where T_{pTx} is the OFDM packet length at the transmitter and T_{pRx} is the OFDM packet length at the receiver. In Fig. 6, curves show that the ICI compensation for our proposed method has better performance compared with result for b computed from Eq. (39).

7. CONCLUSIONS

We consider OFDM signaling over multi-scale multi-lag (MSML) underwater acoustic channels wherein the effect of mobility induces a unique time scaling of the transmitted signal on each channel path resulting in significant intercarrier interference (ICI) at the receiver. The optimal resampling factor which minimizes the power of the ICI at the receiver was determined given the statistical models for the parameters of the MSML channel. First the exact ICI power was determined and then an upper bound to this power was developed which enabled optimization. For the special case of K-state modeling of the scale parameters, the upper-bound was evaluated and optimal resampling factor calculated. Simulation results show that the proposed method and model result in better performance than that of the classical resampling factor computation via comparison of the transmitted and received packet durations. Our current approach assumes a Rayleigh-like model for the channel coefficients; however, recent work [15] suggests that a Ricean model may be more accurate - this is an avenue of future work.

APPENDIX

A. PROOF OF THEOREM 1

From (26), we can write down

$$S_m(f) \leq \left(\sum_{k=-\infty}^{+\infty} \operatorname{sinc}^2\left((\beta f + 1)\, k + (\alpha\beta f - m) \right) \right) - \operatorname{sinc}^2\left(\beta\,(\alpha + m)\, f \right). \quad (40)$$

The first term of the right hand side of (40) can be interpreted as the summation of $f(t) = \operatorname{sinc}^2\left((\beta f + 1)\, t + (\alpha\beta f - m) \right)$ samples at times $t = k$. if we say $F(\Omega)$ is Discrete Fourier Transform (DFT) of $f(k)$, then

$$\sum_{k=-\infty}^{+\infty} f(k) = F(\Omega)|_{\Omega=0}. \quad (41)$$

Using time-shifting property of DFT, we know

$$F(\Omega) = \frac{1}{(\beta f+1)} \sum_{l=-\infty}^{+\infty} e^{j\frac{\alpha\beta f - m}{(\beta f+1)}\Omega} \Lambda\left(\frac{\Omega - 2\pi l}{2\pi\,(\beta f+1)} \right), \quad (42)$$

where $\Lambda(\Omega)$ is triangle function defined as following,

$$\Lambda(\Omega) = \begin{cases} 1 - |\Omega| & |\Omega| \leq 1 \\ 0 & \text{O.W} \end{cases}$$

Using (42) and (41),

$$\begin{aligned} &\sum_{k=-\infty}^{+\infty} \operatorname{sinc}^2\left((\beta f + 1)\, t + (\alpha\beta f - m) \right) \\ &= \left(\frac{1}{\beta f+1} \sum_{l=-\infty}^{+\infty} e^{j\frac{\alpha\beta f - m}{(\beta f+1)}(\Omega - 2\pi l)} \Lambda\left(\frac{\Omega - 2\pi l}{2\pi\,(\beta f+1)} \right) \right) \Bigg|_{\Omega=0} \\ &= \frac{1}{(\beta f+1)} \sum_{|l|<(\beta f+1)} e^{\frac{-j2\pi(\alpha\beta f - m)}{(\beta f+1)} l} \left(1 - \frac{|l|}{(\beta f+1)} \right). \end{aligned} \quad (43)$$

Since the bounds of integration on (27) are specified with $G(f)$ which are f_l and f_u(These values are evaluated from (22)), We approximate the $S_m(f)$ over $f_l \leq f \leq f_u$. For $f_l \leq f < 0$, k can be only equal zero. For $0 \leq f \leq f_u$, k can be equal to 0 and ± 1. Thus, by substituting the k values in (43), the proof is complete.□

B. REFERENCES

[1] S.J. Hwang and P. Schniter, "Efficient communication over highly spread underwater acoustic channels," *in Proc. 2nd Workshop Underwater Netw.*, pp. 11-18, 2007.

[2] T. Kang and R. A. Iltis, "Iterative carrier frequency offset and channel estimation for underwater acoustic OFDM systems," *IEEE J. Sel. Areas Commun.*, vol. 26, no. 9, pp. 1650-1661, Dec. 2008.

[3] B. Li, S. Zhou, M. Stojanovic, L. Freitag, P. Willet, "Multicarrier Communication Over Underwater Acoustic Channels With Nonuniform Doppler Shifts," *IEEE J. Ocean. Eng.*, vol. 33, no. 2, pp. 198-209, April 2008.

[4] S. Yerramalli, U. Mitra, "Optimal Resampling of OFDM Signals for Multiscale Multilag Underwater Acoustic Channels," *IEEE J. Ocean. Eng.*, vol. 36, no. 1, pp. 126-138, Jan. 2011.

[5] S. T. Rickard, R. V. Balan, H. V. Poor, S. Verdú,"Canonical time-frequency, time-scale, and frequency-scale representations of time-varying channels," *International Press of Boston, Communication in Information and Systems*, vol. 5, no. 2, pp. 197-226, 2005.

[6] Y. Jiang, A. Papandreou-Suppappola, "Discrete time-scale characterization of wideband time-varying systems," *IEEE Trans. Signal Process.*, vol. 54, no. 4, pp. 1364-1375, Apr. 2006.

[7] A.F. Molisch, *Wireless communications*, Wiley, 2011.

[8] P. Robertson, S. Kaiser,"The effects of Doppler spreads in OFDM(A) mobile radio systems," *IEEE Veh. Tech. Conf.* (VTC-Fall), vol. 1, pp. 329-333, 1999.

[9] B. Li, S. Zhou, M. Stojanovic, L. Freitag, and P. Willet, "Multicarrier underwater acoustic communications over fast-varying channels," *IEEE J. Ocean. Eng.*, vol. 33, no. 2, pp. 198-209, Apr. 2008.

[10] B. Li, J. Huang, S. Zhou, K. Ball, M. Stojanovic, L. Freitag, and P. Willet, "Further results on high-rate

MIMO-OFDM underwater acoustic communications," *in Proc. MTS/IEEE OCEANS Conf.*, Quebec City, QC, Canada, Sep. 2008.

[11] S. Mason, C. R. Berger, S. Zhou, K. R. Ball, L. Freitag, and P. Willett, "Receiver comparisons on an OFDM design for Doppler spread channels," *in Proc. MTS/IEEE OCEANS Conf.*, May 2009.

[12] A.R. Margetts, P. Schniter, A. Swami, "Joint scale-lag diversity in wideband mobile direct sequence spread spectrum systems," *IEEE Trans. Wireless Commun.*, vol. 6, no. 12, pp. 4308-4319, Dec. 2007.

[13] M. Stojanovic, "Low complexity OFDM detector for underwater acoustic channels," *in Proc. IEEE/MTS OCEANS Conf.*, Sep. 2006.

[14] B. S. Sharif, J. Neasham, O. R. Hinton, and A. E. Adams, "A computationally efficient Doppler compensation system for underwater acoustic communications," *IEEE J. Ocean. Eng.*, vol. 25, no. 1, pp. 52-61, Jan. 2000.

[15] P. Qarabaqi, M. Stojanovic, "Statistical modeling of a shallow water acoustic communication channel," *Proc. Underwater Acoustic Measurements Conference, Nafplion, Greece, 2009.*

[16] F. Hlawatsch, G. Matz, *Wireless communications over rapidly time-varying channels*, Academic Press, 2011.

[17] A. Papoulis, *Probability, random variables, and stochastic processes*, McGraw-Hill, 2000.